THE TWO-DIMENSIONAL POLYNOMIAL LEAST SQUARES (*PoLeS*) FILTER : A METHOD FOR REDUCING HIGH AND LOW VALUE NOISE IN SATELLITE DATA

Jose Edgardo L. ABAN*
Ryutaro TATEISHI**

*Center for Environmental Remote Sensing (CEReS)
Chiba University
1-33 Yayoi, Inage, Chiba-ken, Japan
Tel: +81-43-290-3965 Fax: +81-43-290-3857
E-mail: aban@ceres.cr.chiba-u.ac.jp
JAPAN

**Center for Environmental Remote Sensing (CEReS)
Chiba University
1-33 Yayoi, Inage, Chiba-ken, Japan
Tel: +81-43-290-3965 Fax: +81-43-290-3857
E-mail: aban@ceres.cr.chiba-u.ac.jp
JAPAN

KEY WORD: Polynomial least squares, filtering, noise, convolution

ABSTRACT:

A *Polynomial Least Squares Operation* (*PoLeS*) 5X5 two-dimensional filter consisting of filter coefficients was applied to the following data: (1) SPOT data which was artificially contaminated with low and high value noise pixels; (2) single channel (channel 7) LANDSAT TM with systematic noise; (3) PAL NOAA-AVHRR NDVI cloud-contaminated data; (4) raw, speckled JERS -1 data, in order to test the efficacy of the *PoLeS* method in filtering out both low and high value noise. The method showed substantial reduction of noise in the *PoLeS*-filtered data values, with an overall smoothing effect on the image but with moderate preservation of edges, upon visual examination. The *PoLeS* Method is likewise compared with the classical or convolution filtering techniques such as the average, median and mode filters.

The *PoLeS* filter is proposed as an alternative and novel noise filtering technique that can be applied to a number of satellite data, to reduce high and low value noise.

1. INTRODUCTION

Image enhancements of most interest in remote sensing generally relate to smoothing, edge detection and enhancement, and line detection. Likewise, image enhancements are made to restore images that suffer from errors, noise, and geometric distortion introduced into the data during the scanning, transmission, and recording processes (Sabins, 1987). There are two basic types of noise in image data, random and nonrandom noise. Periodic line dropouts and striping are forms of nonrandom noise. Random noise occurs as individual pixels with digital numbers (DNs) that are much higher or lower than the surrounding pixels (Sabins, 1987). This will often show as a speckled “salt and pepper” pattern on the image in regions of homogeneity; it can be removed by the process of low pass filtering or smoothing, unfortunately at the expense of some high frequency information in the image (Richards, 1986). Nonrandom noise on the other hand include periodic line drop-outs and stripping.

Most of methods for noise removal in digital images are template techniques, in which a template or a filter, box or window is defined and then moved over the image row by row and column by column. The product of the pixel brightness values, covered by the template at a particular position, and the template entries are taken and summed to give the template response. This response is then used to define a new brightness value for the pixel currently at the center of the template. When this is done for every pixel in the image, a radiometrically modified image is produced that enhances or smoothens geometric features according to the specific numbers loaded into the template.

Digital filters have been used to derive these values. Filtering provides a means of improving images by suppressing or enhancing certain spatial frequencies, directions an textures (Rosenfeld and Kak, 1976) The earliest examples involve a three by three array which substitutes the central pixel of the array with a simple measure of digital number variance (range, kurtosis, standard deviation) as it passes over the image (Haralick et al. 1973, Logan et al. 1979). These have proved to be particularly useful for a number of operations like the smoothing out of over enlarged discrete images to make them appear continuous; the suppression of banding that is common to both Landsat MSS and TM images and the suppression of "speckle" in radar images (Lee, 1981; Bruniquel et al, 1997; Gineste, 1999; Frulla et al, 2000; Ndi Nyoungui et al, 2002; and Dekker, 1998). Likewise, filters have been used for a menagerie of applications, to wit, image sharpening or edge enhancement (Short, 1982), geological mapping (Thomas et al. 1981), terrain analysis (Weszka et al. 1976; Shih and Schowengerdt, 1983), land cover mapping (Hsu, 1978; Irons and Petersen, 1981), forest mapping (Logan et al, 1979), urban classification (Jensen, 1981) and the differentiation of sea ice (Gersen and Rosenfeld 1975) and clouds (Harris, 1977).

The *Polynomial Least Squares Operation* (*PoLeS*), which had been applied to the smoothing of AVHRR NDVI annual profile (Aban et al, 2002), is just as useful for array or two dimensional data processing. The process involves fitting a two-dimensional polynomial to a two-dimensional array of data, either for derivation of numerical derivatives or smoothing of image.

The *PoLeS* Method is applied to a number of satellite data sources and noise contaminated data, in order to test the technique's efficiency and viability in restoring or enhancing the quality of the image data.

2. PRINCIPLE OF THE TWO-DIMENSIONAL POLYNOMIAL LEAST SQUARES OPERATION (*PoLeS*)

Consider a two-dimensional 5X5 data array. The data may be laid out as in below:

		x_i				
		-2	-1	0	1	2
	-2	g(0)	g(1)	g(2)	g(3)	g(4)
	-1	g(5)	g(6)	g(7)	g(8)	g(9)
y_i	0	g(10)	g(11)	g(12)	g(13)	g(14)
	1	g(15)	g(16)	g(17)	g(18)	g(19)
	2	g(20)	g(21)	g(22)	g(23)	g(24)

g(i) is the pixel value, and the column vector g represents the all the array data, in which case,

$$g = \{g(0)\ g(1) \ldots g(24)\}^T \tag{1}$$

Fitting a third order, two-dimensional polynomial to this array, we have

$$g(i) \quad f(x_i,y_i) = a_{00} + a_{10}x_i + a_{01}y_i + a_{20}x_i^2 + a_{11}x_iy_i + a_{02}y_i^2 + a_{30}x_i^3 + a_{21}x_i^2y_i + a_{12}x_iy_i^2 + a_{03}y_i^3$$

Here (x_iy_i) is the coordinate of the pixel of g(i) It can be noted that the coefficients of x^iy^j is a_{ij}. The coefficients can be computed by performing a matrix procedure, with the matrix equation:

$$Xa=g \tag{2}$$

Where

$$X = \begin{bmatrix} 1 & x_0 & y_0 & x_0^2 & x_0y_0 & y_0^2 & x_0^3 & x_0^2y_0 & x_0y_0^2 & y_0^3 \\ 1 & x_1 & y_1 & x_1^2 & x_1y_1 & y_1^2 & x_1^3 & x_1^2y_1 & x_1y_1^2 & y_1^3 \\ \vdots & \vdots & \vdots & \vdots & \vdots & \vdots & \vdots & \vdots & \vdots & \vdots \\ 1 & x_{24} & y_{24} & x_{24}^2 & x_{24}y_{24} & y_{24}^2 & x_{24}^3 & x_{24}^2y_{24} & x_{24}y_{24}^2 & y_{24}^3 \end{bmatrix}$$

and **a** is the vector of polynomial coefficients:

$$\underline{a} = (a_{00}a_{10}a_{01}a_{20}a_{11}a_{02}a_{30}a_{21}a_{12}a_{03})^T \tag{3}$$

Equation (1) reproduces the polynomial for each of the values in the array of data. The polynomial coefficients can be solved by employing the least squares operation.

$$A= (X^TX)^{-1}X^Tg \tag{4}$$

$C = (X^T X)^{-1} X^T$ may be treated as the pseudo-inverse of X, which could be said to be independent of the array data. Each coefficient of the polynomial may be computed as the inner product of one column of pixel values g, and one row of C. The polynomial coefficients may be computed using a linear filter on the array data. By doing so, one can reconstruct g back into a rectangular patch of pixels. Likewise each row of C can be reconstructed into the same size rectangle to derive at a conventional-looking image filter.

Computing for the first three polynomial coefficients we have the following below. It is assumed that coefficient a_{ij} is computed from rectangular filter C_{ij}. As such, the following filter coefficients are produced:

$$C_{00} = \begin{matrix} -0.0743 & 0.0114 & 0.0400 & 0.0114 & -0.0743 \\ 0.0114 & 0.0971 & 0.1257 & 0.0971 & 0.0114 \\ 0.0400 & 0.1257 & 0.1543 & 0.1257 & 0.0400 \\ 0.0114 & 0.0971 & 0.1257 & 0.0971 & 0.0114 \\ -0.0743 & 0.0114 & 0.0400 & 0.0114 & -0.0743 \end{matrix}$$

$$C_{10} = \begin{matrix} 0.0738 & -0.0119 & -0.0405 & -0.0119 & 0.0738 \\ -0.1048 & -0.1476 & -0.1619 & -0.1476 & -0.1048 \\ 0 & 0 & 0 & 0 & 0 \\ 0.1048 & 0.1476 & 0.1619 & 0.1476 & 0.1048 \\ -0.0738 & 0.0119 & 0.0405 & 0.0119 & -0.0738 \end{matrix}$$

$$C_{01} = \begin{matrix} 0.0738 & -0.1048 & 0 & 0.1048 & -0.0738 \\ -0.0119 & -0.1476 & 0 & 0.1476 & 0.0119 \\ -0.0405 & -0.1619 & 0 & 0.1619 & 0.0405 \\ -0.0119 & -0.1476 & 0 & 0.1476 & 0.0119 \\ 0.0738 & -0.1048 & 0 & 0.1048 & -0.0738 \end{matrix}$$

In applying these image patches we are theoretically fitting a two-dimensional polynomial to the array of data surrounding each pixel and then assessing this polynomial.

The coordinate system that is employed in this case is that shown above, where $(x,y) = (0,0)$ at the pixel of interest, which is theoretically in the middle of the data array, in this case the array coordinate g(12). Hence, to calculate the filtered value of the pixel, the polynomial can be evaluated at that point, (x,y) = (0,0). The operation would mean evaluating the polynomial at a_{00}, which can be calculated by applying the 5x5 filter C_{00} to the array of data.

The partial derivatives of the fitted polynomial can likewise be calculated, and applied to the array of data. Below are the partial derivatives:

$$f_x(x_i,y_i) = a_{10} + 2a_{20}x_i + a_{11}y_i + 3a_{30}x_i^2 + 2a_{21}x_iy_i + a_{12}y_i^2 \quad (5)$$

$$f_y(x_i,y_i) = a_{01} + a_{11}x_i + 2a_{02}y_i + a_{21}x_i^2 + 2a_{12}x_iy_i + 3a_{03}y_i^2 \quad (6)$$

Evaluating at $(x,y)=(0,0)$, the outcome are $fx(0,0) = a10$ and $fy(0,0) = a01$, which can be calculated with filters C_{10} and C_{01}.

3. RESULTS AND DISCUSSIONS

The derived 5X5 array coefficients were inputted into the PCI Image processing software through its FILTER facility, applying them onto different data satellite sources.

3.1 Overall Visual Quality

Visual examination of the different filtered images would show distinct changes in both raw and filtered products and would reveal considerable image smoothening in all of the algorithms.

The JERS-1 raw image has a very speckled nature. With subsequent filtering however, there could be observed substantial smoothing in all images. The mode-filtered images have a particularly blotchy and almost “blocky” appearance. This is because the mode filtering algorithm considers the greatest

frequency of brightness values. Examining the raw brightness value of the said images would show that indeed the DN values of the mode-filtered images are mostly of the same ranges in values.

Comparing the *PoLeS*–filtered with that of the mean and median-filtered images would show that although there is an apparent removal of noise by value smoothing, however, the *PoLeS* method preserves most of the edges. This effect is evident in all the four test satellite images.

The reduction in image sharpness may not be as similar as that which can be seen with the Landsat images taken over areas in Jordan. The sixteenth line drop-outs which is more apparent in the channel 7 (thermal) is still apparent in all the images filtered with the different templates. This can be explained by the fact that the standard deviation values have not been significantly changed from its original value of 8.742, by the various filtering methods.

The NOAA images of August 1984 are of particular interest in this study, because of the fact that said images contain systematic noise. In the upper western regions of the African continent can be seen vestiges of high value
noise, left by the daily compositing process. These appear as strips of white pixels.

Similar results can be visually observed with the application of the various filter types on NOAA-AVHRR NDVI data. Visually, there is substantial removal of the high value noise in the mean, median and mode filtered images, with the apparent complete removal of high value noise. However, upon examination of the actual filtered NDVI values and the respective standard deviation values, it could be revealed that the *PoLeS* method lowers the over-all variability of the image data. The original standard deviation of the raw image data is 0.6320, while that of the *PoLeS*-filtered image is 0.406.

3.2 Behavior of Standard deviation and effect on Image Data Variability

Table 1 shows the values of the minimum, maximum and standard deviations of image data, filtered through different means, to wit, median, mean, mode and *PoLeS* methods. In all cases, substantial reduction of image variability can be observed, as shown by the tapering value of the standard deviations.

The standard deviations of *PoLeS*-filtered data are lowest for Landsat, JERS-1 NOAA datasets, indicating that the overall variability inherent in the original data are diminished. The plots of the mean, maximum, and minimum values shown in Figure 6 would clearly show this tapering in the overall values of the standard deviation, as a consequence of changes in the overall data maxima and minima after filter with *PoLeS*.

SPOT DATA WITH GAUSSIAN NOISE	RAW	MEAN FILTERED	*PoLeS* FILTERED	MEDIAN FILTERED	MODE FILTERED
COMPUTED AVERAGE	127.616	127.617	121.742	128.232	123.764
STANDARD DEVIATION	24.537	14.459	16.779	14.977	19.972
MINIMUM VALUE	0	74	45.19	71	0
MAXIMUM VALUE	255	182	190.67	184	255

(a)

LANDSAT DATA	RAW	MEAN FILTERED	*PoLeS* FILTERED	MEDIAN FILTERED	MODE FILTERED
COMPUTED AVERAGE	90.9630	90.9630	86.77	90.879	90.352
STANDARD DEVIATION	8.742	8.156	8.105	8.281	8.608
MINIMUM VALUE	36	44	37.43	42	42
MAXIMUM VALUE	131	125	121.19	125	126

(b)

JERS-1 DATA	RAW	MEAN FILTERED	*PoLeS* FILTERED	MEDIAN FILTERED	MODE FILTERED
COMPUTED AVERAGE	37.0300	39.166	25.370	37.030	33.459
STANDARD DEVIATION	21.094	22.352	15.509	21.094	24.368
MINIMUM VALUE	6	8	0	6	0
MAXIMUM VALUE	243	226	165	243	255

(c)

NOAA NDVI DATA	RAW	MEAN FILTERED	*PoLeS* FILTERED	MEDIAN FILTERED	MODE FILTERED
COMPUTED AVERAGE	-0.412	-0.412	-0.267	-0.413	-0.426
STANDARD DEVIATION	0.6320	0.624	0.406	0.630	0.630
MINIMUM VALUE	-1.016	-1.016	-0.9364966	-1.016	-1.016
MAXIMUM VALUE	0.99200	0.79	0.6716253	0.816	0.992

(d)

Table1. Shows the changes in the overall image statistics, as measured by the change in the value of the image mean before and after filtering processes; (a) SPOT;(b) LANDSAT; (c) JERS-1; and (d) NOAA-AVHRR. Note that for a, b, and c the values represent brightness (DN) values, while for d the actual NDVI values (ranging from –1 to +1).

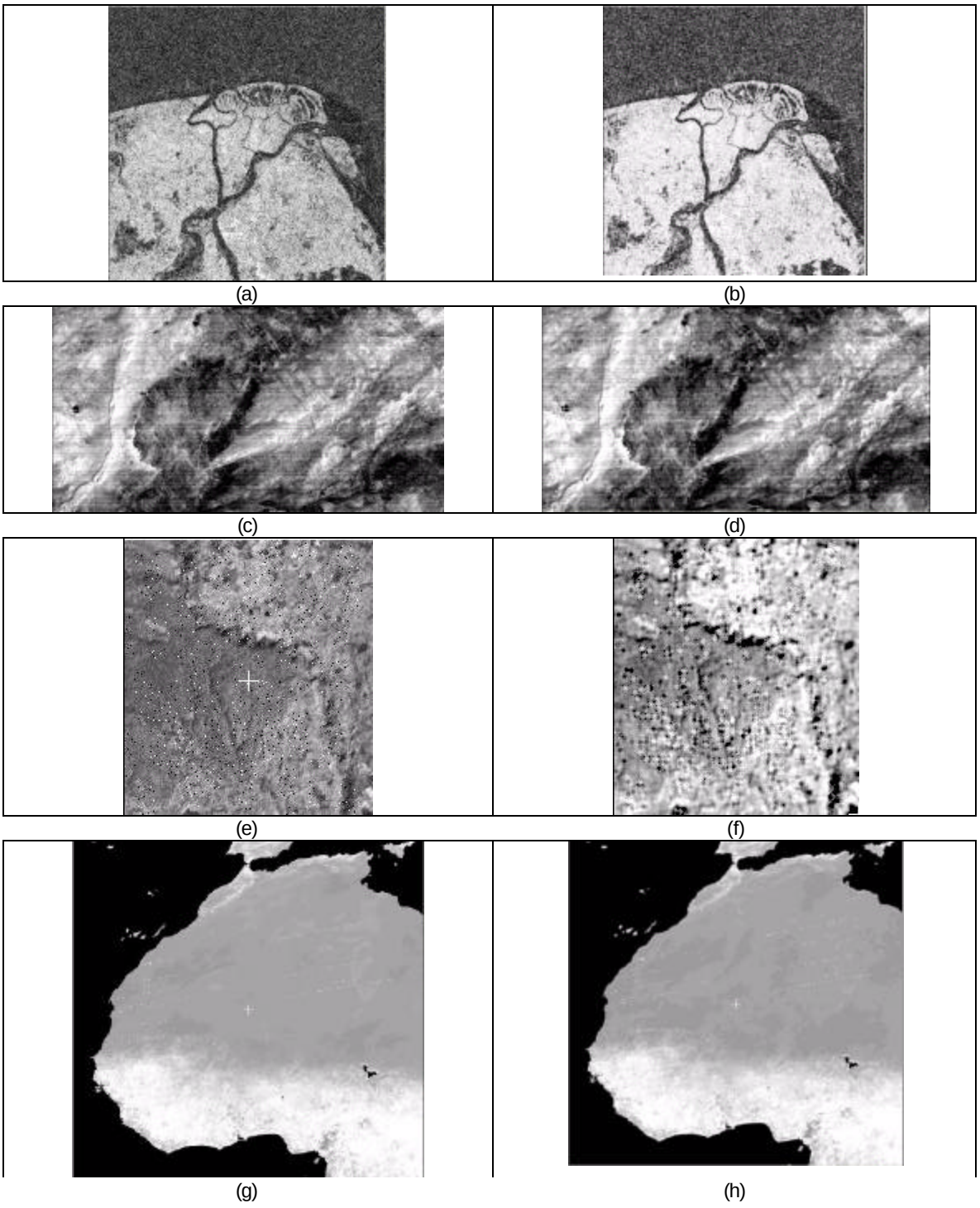

Fig. 1. Illustration of the effect of *PoLeS* filtering on different image sources (a) original image of JERS-1 over Panay Island Philippines; (b) filtered image; (c) original image of LANDSAT over Jordan; (d) filtered image; (e) SPOT with Gaussian noise; (f) filtered image; (g) NOAA-AVHRR NDVI image over western Africa with systematic noise; (h) filtered image

4. CONCLUSIONS

The *PoLeS* two-dimensional filter is comparatively effective in reducing high and low value noise in satellite image data, as that of the conventional/traditional filters, to wit, the mean, median, and mode filters.

The over-all effect of the *PoLeS* filter is that of image smoothing, thereby generally, lowering the overall variability inherent in the original image data, as shown by the change (lower) in the standard deviation values of the *PoLeS*-filtered. Visually, *PoLeS*-filtered images are smoothened images. However, as compared to mean- and mode -filtered images, the *PoLeS* moderately preserves edges.

While this research has focused on the effect of *PoLeS* filtering on two-dimensional data, future research can be made to assess the *PoLeS* filter's effects in the classification and accuracy of the classified satellite image products.

REFERENCES

Aban, J.E.L. Tateishi R. and Tsolmon R. (2002) The Polynomial Least Squares Operation (*PoLeS*): A Method for Reducing Noise in NDVI Time Series Data IEEE Letters. Taylor and Francis Ltd. (*in press*)

Bjorck, A. (1996) Numerical methods for least squares problems SIAM.

Bruniquel, J. and Lopes A. (1997) Multi-variate optimal speckle reduction in SAR imagery. International Journal of Remote Sensing, 18: 603-27.

Dekker, R.J. (1998) Speckle filtering in satellite SAR change detection imagery. International Journal of Remote Sensing, 19: 1133-46.

Farebrother, R.W. (1988) Linear least squares computations. Marcel Dekker Statistics, textbooks and monographs , Vol. 91.

Frulla, L.A. Milovich J.A. and Gagliardini D.A. (2000) Automatic computation of speckle standard deviation in SAR images. International Journal of Remote Sensing, 21: 2883-99.

Gersen, D.J. and Rosenfeld, A. (1975) Automatic sea ice detection in satellite pictures. Remote sensing of Environment. 4: 187-98.

Gineste, P. (1999) A simple, efficient filter for multi-temporal SAR images. International Journal of Remote Sensing, 20: 2565-76.

Haralick, R.M., Shanmugam, K.S. and Dinstein, I. (1973) Textural Features for Image Classification. IEEE Transactions on Systems, Man and Cybernetics, 3: 610-21.

Harris, R. (1977) Automatic analysis of meteorological satellite imagery In Thomas J.O. and Davey P.G. (eds.) Texture Analysis. British Pattern Recognition Association and Remote Sensing Society, Reading, pp. 45-72.

Hsu, S. (1978) Texture tone analysis for automated land use mapping. Photogrammetric Engineering and Remote Sensing, 44: 1393-404.

Irons, J.R. and Petersen, G.W. (1981) Texture transforms of remote sensing data. Remote Sensing of the Environment, 11: 359-70.

Jensen, J.R. (1981) Urban change detection mapping using Landsat digital data. The American Cartographer, 8: 127-47.

Lawson, C.L. and Hanson R.J. (1974) Solving least squares problems. Prentice-Hall.

Lee, J. (1981) Speckle analysis and smoothing of synthetic aperture radar images. Computer Graphics and Image Processing, 17:24-32.

Logan, T.L., Strahler, A.H. and Woodcock, C.E. (1979) Use of a standard deviation based texture channel for Landsat classification of forest strata. Machine Processing of Remotely Sensed Data Symposium. Purdue University, Indiana, pp. 395-404.

Lohmoller, J.B. (1989) Latent variable path modeling with partial least squares. Physica-Verlag.

Macchi, O. (1995) Adaptive processing : the least mean squares approach with applications in transmission. John Wiley & Sons.

Ndi Nyoungui A. , Tonye E. and Akono A. (2002) Evaluation of speckle filtering and texture analysis methods for land cover classification from SAR images. International Journal of Remote Sensing, 23: 1895-1925.

Richards, J.A. (1986). Remote Sensing Digital Image Analysis : An Introduction. Sprinegr-Verlag. New York.

Rosenfeld, A. and Kak, A.C. (1976) Digital Picture Processing. Academic Press, New York.

Rao, C.R. and Toutenburg, H. (1995) Linear models : least squares and alternatives. Springer.

Shi, E.H. H. and Schowengerdt, R.A. (1983) Classification of arid geomorphic surfaces using spectral and textural features. Photogrammetric Engineering and Remote Sensing

Short, N.M. (1982) The Landsat Tutorial Workbook: Basics of Satellite Remote Sensing. National Aeronautics and Space Administration Reference Publication 1078, Washington DC.

Ten Berge, J.M.F. (1993) Least squares optimization in multivariate analysis DSWO Press, Leiden University.

Thomas, I.L. Howorth R., Eggers A.E. and Fowler A.D.W. (1981) Textural Enhancement of a circular geological feature. Photogrammetric Engineering and Remote Sensing, 47:89-91

Weszka, J.S., Dyer, C.R. and Rosenfeld, A. (1976) A comparative Study of texture measures for terrain classification. IEEE Transactions on Systems, man and Cybernetics, 6: 269-85.